Electrochimica Acta 130 (2014) 164–169

Contents lists available at ScienceDirect

Electrochimica Acta

journal homepage: www.elsevier.com/locate/electacta

Electrochemical and in-situ stm study of the surface alloy formation in the system Au(100)/Cd

M.C. del Barrio, D.R. Salinas[†], S.G. García[*,1]

Instituto de Ing. Electroquímica y Corrosión (INIEC), Departamento de Ingeniería Química, Universidad Nacional del Sur, Avda. Alem 1253, (8000) Bahía Blanca, Argentina

ARTICLE INFO

Article history:
Received 5 January 2014
Received in revised form 24 February 2014
Accepted 25 February 2014
Available online 11 March 2014

Keywords:
Alloy formation
Cd UPD
Au(100)
in-situ STM

ABSTRACT

The Cd UPD process in the system Au(100)/Cd^{2+}, SO_4^{2-} and the involved Au-Cd surface alloy formation have been investigated, using conventional electrochemical techniques and in-situ STM analysis. The voltammetric experiences have shown three adsorption/desorption steps in the extended UPD range $0 \leq \Delta E/mV \leq 800$. The obtained desorption spectra indicate the formation of a surface alloy at low underpotentials and long polarization times. STM images have shown that the Cd deposition becomes evident at low underpotentials, with the nucleation of two-dimensional islands of monatomic height, which grow and coalesce up to a complete monolayer. At lower underpotentials, new islands nucleate on the monolayer previously formed, and grow acquiring a quadratic structure. The subsequent stripping of this film promotes morphological changes that are related to the dissolution of a Cd-Au surface alloy, which is consistent with the electrochemical experiences.

1. Introduction

Cd presents a relatively more negative standard potential than most metals, allowing a relatively large selection of substrates for investigating underpotential deposition (UPD) processes. In addition, the hydrogen overpotential on this metal is high enough, so that the hydrogen evolution reaction practically does not occur on the Cd layers formed by UPD [1].

The Cd UPD on gold substrates appears as an interesting process due to its promising application for high quality thin film semiconductor devices [2] and its catalytic properties for some relevant electrochemical reactions, such as the electroreduction of nitrate anions and other nitrogen compounds [3,4]. Furthermore, Cd is known to produce intermetallic phases on Au in the UPD region during long time polarization experiments [5].

Particularly, the Cd UPD onto Au(111) has been the subject of numerous and contrasting studies [1,5–9], but on the other hand, the Cd UPD on the Au(100) substrate, was only studied by Vidu, R. and Hara, S. [10–13], by cyclic voltammetry and Atomic Force Microscopy (AFM). Based on their experiences, they demonstrated that the Cd UPD on Au (100) involves several sorption steps evidenced by two adsorption/desorption peaks pairs in the cyclic voltammogram before the peaks pair corresponding to the Cd bulk deposition and stripping. The deposition begins with the formation of an expanded Cd adlayer with a $(\sqrt{2}x\sqrt{2})R45^\circ$ structure, which is then transformed into a (1×1) condensed one. A Au-Cd surface alloy was proposed at lower underpotentials, formed by a place exchange process, between the adsorbed Cd atoms and the underlying Au atoms. The authors noted that this process occurs on flat terraces but not on the step edges, preserving the morphology of the flat surface. They proposed that surface alloying consisted of two processes. A first one relatively fast limited to a few monolayers and evidenced by the rapid charge increase at short polarization times. This process was associated with a vertical atomic place exchange between the adsorbate and the substrate atoms and characterized by a diffusion coefficient $D_1 \approx 10^{-16}$ cm^2 s^{-1}. The second process, which occurs more distant from the surface and at long polarization times, was characterized by a diffusion coefficient $D_2 \approx 10^{-18}$ cm^2 s^{-1}. This phenomenon was related to a slow solid state diffusion of the Cd or the Au atoms, across the recently formed alloy film.

Vidu, R. and Hara, S. [10,14] have also studied the Cd deposition on Au(100) at low overpotentials by AFM, reporting the nucleation and growth of islands on the terraces and step edges. The Cd layers follow the Stranski-Krastanov growth mechanism, which

* Corresponding author. Tel.: +54 291 4595182; fax: +54 291 4595182.
E-mail address: sgarcia@criba.edu.ar (S.G. García).
[1] ISE member.
[†] Deceased.

http://dx.doi.org/10.1016/j.electacta.2014.02.143
0013-4686/

begins with a Cd monolayer formation and continues in an island growth mode, where the Cd deposit follows the Au (100) substrate orientation.

The aim of the present paper is to get further insight into the Cd UPD process in the system Au(100)/Cd^{2+}, SO_4^{2-}, taking into account the morphological changes during the Cd adsorption/desorption processes as well as the Au-Cd surface alloying. In this sense, the work is focussed on the formation of the Au-Cd surface alloy at underpotentials, using conventional electrochemical techniques and in-situ STM analysis.

2. Experimental

The experiments were performed in the system Au(100)/Cd^{2+}, SO_4^{2-} using a Au(100) single crystal electrode with a diameter of 0.4 cm. The substrate surface was first mechanically polished with diamond paste of decreasing grain size down to 0.25 μm and subsequently electrochemically polished in a cyanide bath according to a standard procedure [15]. This pre-treatment procedure prior to each measurement was already previously described [16].

The electrolyte solution used throughout the study was 5 mM H_2SO_4 + 0.1 M Na_2SO_4 + 1 mM $CdSO_4$. This solution was prepared from suprapure chemicals (Merck, Darmstadt) and fourfold quartz-distilled water, and deareated by nitrogen bubbling prior to each experiment.

Conventional electrochemical studies were performed in a standard three-electrode electrochemical cell. The counter electrode was a platinum sheet (1 cm^2) and the reference electrode was a $Hg/Hg_2SO_4/K_2SO_4$ saturated electrode (SSE), mounted inside a Luggin capillary. The actual electrode potential, E, is referred to the SSE, whereas the underpotential, ΔE, is related to the Nernst equilibrium potential of the 3D Cd phase by $\Delta E = E - E_{3DCd}$, with E_{3DCd} = -1150 mV for $c_{Cd^{2+}}$ = 1 mM. The measurements were carried out with a potentiostat-galvanostat EG&G Princeton Applied Research Model 273A.

A standard Nanoscope III equipment (Digital Instruments, Santa Barbara, CA, USA) was used for the in-situ STM studies, employing Apiezon insulated Pt-Ir tips (Digital Instruments, Santa Barbara, USA). Pt wires were used as counter- and quasi-reference electrode. The potentials of the gold substrate and the STM tip were controlled independently by a Nanoscope III-bipotentiostat optimised for the STM set-up used. The tip potential was held constant at a value of minimum faradaic current and the tip current varied in the range $2 \leq I_{tun}/nA \leq 20$. The experimental set-up for the in-situ STM technique has been checked by cyclic voltammetric measurements and the results were identical to those obtained in the conventional electrochemical cell.

3. Results and Discussion

3.1. Electrochemical experiments

Fig. 1 shows the cyclic voltammogram obtained for the system Au(100)/Cd^{2+}, SO_4^{2-}. The Cd UPD on Au(100) is clearly observed in the underpotential range $0 \leq \Delta E/mV \leq 800$, where two different adsorption/desorption current density peaks were exhibited. The first peaks pair is located at $\Delta E_{A1/D1} \approx 650$ mV, and the second one at $\Delta E_{A2} \approx 205$ mV and $\Delta E_{D2} \approx 340$ mV, in agreement with those reported by other authors [10–13]. Another adsorption/desorption peaks pair ($\Delta E_{A3} \approx 90$ mV/$\Delta E_{D3} \approx 210$ mV) at underpotentials close to the equilibrium potential was also recorded, which were not previously reported.

In order to further explore the non-equilibrium phenomenon of Cd-Au surface alloying, long time polarization experiments were performed. In this case, a freshly Au surface was used for each

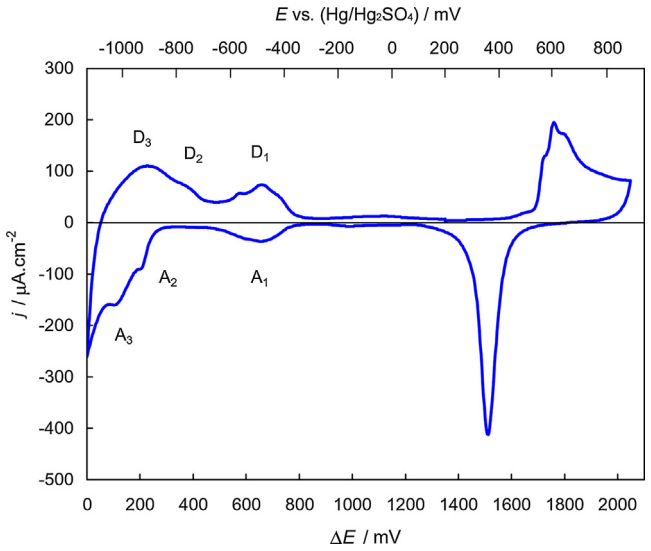

Fig. 1. Cyclic voltammogram for the system Au(100)/5 mM H_2SO_4 + 0.1 M Na_2SO_4 + 1 mM $CdSO_4$. T = 298 K, $|dE/dt|$ = 50 mV s^{-1}.

of the sweeps. The potential was stepped from ΔE = 1700 mV, an underpotential value between the peak D_1 and the oxidation of the substrate, to different underpotentials ΔE_p up to the onset of Cd bulk deposition. After maintaining the selected ΔE_p value for different polarization times, t_p, the potential was swept back recording the corresponding ΔE-i desorption spectra (Fig. 2). After the polarization at ΔE_p = 750 mV, i.e. the initial region of Cd UPD, no significant changes in the registered desorption curves were recorded (curves not shown), indicating that no irreversible processes related to Cd adsorption take place. After the polarization at ΔE_p = 550 mV and for long polarization times (Fig. 2.a), some irreversibility related to the Cd deposit begins to evidence, given by the appearance of an additional peak, D'. Moreover, the peak D_1 does not remain stable and its height decreases with t_p. This effect is accentuated for ΔE_p = 250 mV (Fig. 2.b), where it is clearly shown that the peak D' is increased with the polarization time. However, with increasing t_p the peak D_1 decreases significantly in height. At ΔE_p = 150 mV (Fig. 2.c) the desorption spectrum shows two additional stripping peaks, D" and D"', in the underpotential range $1150 \leq \Delta E/mV \leq 1500$, for relatively long polarization times (t_p = 1800 s). Finally, at ΔE_p = 100 mV (Fig. 2.d), a significant increase in the height of the peaks D_3 and D"' is observed. From these curves it is possible to confirm the formation of a Au-Cd alloy, which involves different phases, given by the appearance of new peaks. All these new peaks were not previously reported by other authors.

The time-dependence of the stripping charge density, Δq, is reported in order to analyze the possible steps during the Au-Cd alloy formation (inset of Fig. 2 for each underpotential value). Δq was obtained by integrating the anodic current density over the potential ranges at which the desorption curves (Fig. 2a-d) were recorded, i.e. from ΔE_p to 1500 mV. ΔE_p values are indicated in each inset plot of the Fig. 2. It is known that a lineal relation between Δq and $t_p^{1/2}$ is an evidence of a solid state diffusion alloy formation mechanism [5,8,17]. The first portion of the plots (dashed lines) corresponds to the adsorption stage together with the intermixing at the interface [12], and it is beyond the aim of our study. We are interested in the processes at long polarization times where the formation of a Au-Cd alloy involving solid state diffusion takes place. At ΔE_p = 550 mV, the desorption charge density remains nearly constant with $t_p^{1/2}$. Nevertheless, some changes were recorded in the

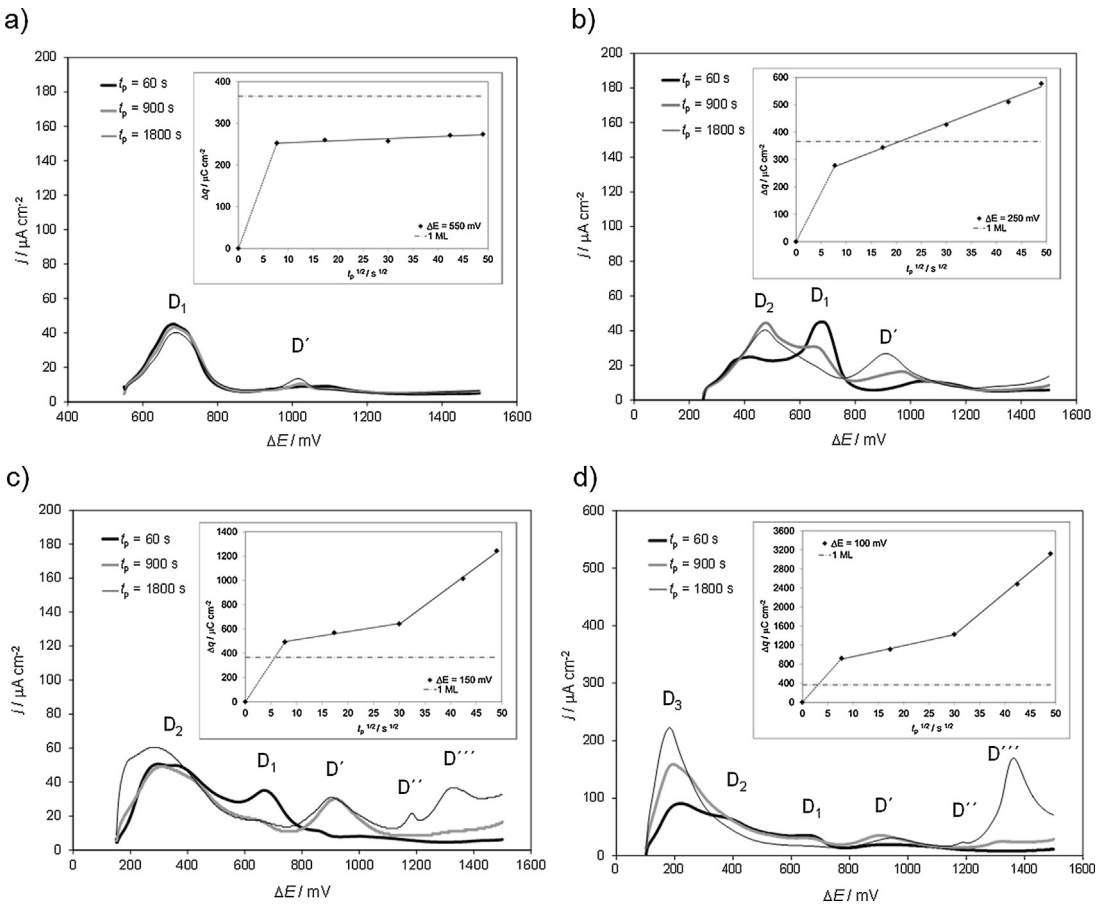

Fig. 2. Current-potential desorption spectra obtained in the system Au(100)/1 mM $CdSO_4$ + 5 mM H_2SO_4 + 0.1 M Na_2SO_4, after polarization during different times at: a) ΔE_p = 550 mV, b) ΔE_p = 250 mV, c) ΔE_p = 150 mV, d) ΔE_p = 100 mV. T = 298 K, $|dE/dt|$ = 50 mV s^{-1}. Inset: Relation Δq - $t_p^{1/2}$, for each underpotential value.

desorption curves (cf. Fig. 2.a), by the appearance of an additional peak (D'), indicating the occurrence of surface transformations associated with an atomic place exchange process between Au substrate atoms and Cd atoms recently deposited. At ΔE_p = 250 mV, the changes are more pronounced (cf. Fig. 2.b), and the stripping charge density value exceeds that required for the formation of a completely closed packed Cd monolayer onto Au(100) ($\Delta q_{ML} \approx$ 365 µC cm^{-2}). This fact could be explained considering that after the vertical atomic place exchange process, Au atoms reach the interface electrode/electrolyte and act as new sites available for Cd adsorption. Thus, the number of Cd atoms deposited in the underpotential range is not limited to a monolayer, and increases with the polarization time. For relatively long polarization times, the extent of the alloyed phase into the surface will be governed by solid state diffusion of both Cd and Au atoms through the alloy surface rich in vacancies. In the underpotential range 100 < ΔE_p/mV < 150, the corresponding anodic charge density, Δq, considerably exceeds the value of a Cd monolayer and increases significantly with t_p, exhibiting two different linear Δq - $t_p^{1/2}$ dependences, for relatively short and long polarization times. The behavior observed at short polarization times, is attributed to the formation of an initial thin alloy film by a turnover mechanism. A similar model was already proposed for this system [11,12], and also for Ag(100)/Cd [13] and Ag(111)/Cd [18]. This initial formation of the Au-Cd surface alloy is followed by a second and more pronounced anodic charge density increase at higher t_p, reflected in the appearance of the peaks D" and D"' in the anodic stripping curves, which can be attributed to the formation of other phases of a Cd_zAu_x alloy [17].

3.2. In-situ STM studies

Cd electrodeposition onto Au(100) and the involved Au-Cd alloy was also studied by in-situ STM (Fig. 3). Fig. 3.a shows the initial free Au(100) substrate surface at ΔE = 1250 mV, where no faradaic process takes place. The surface consists of atomically smooth terraces separated by monatomic steps and some 2D Au islands. The high step density is related to the etching pre-treatment used, in agreement with previous results obtained for Au(111) [19] and Au(100) [16]. This surface morphology gradually changes when the potential is shifted to more negative values, up to ΔE = 950 mV (E = -200 mV vs SSE), due to a surface diffusion process of the mobile Au atoms (Fig. 3.b). This high surface mobility was also reported for this substrate by Hara et al. [20] and by Salinas et al. for Au(111) [19]. Cd UPD can be recognized more clearly if particular attention is paid in the contoured region of Fig. 3b. No surface morphology changes are observed in the potential range 250 ≤ ΔE/mV ≤ 800 where the A_1/D_1 Cd UPD peaks are recorded. At ΔE = 200 mV, in the A_2/D_2 peaks pair region, 2D islands are formed on top of the flat terraces and step edges (Fig. 3.c), which grow and coalesce (Fig. 3.d). At lower underpotentials, ΔE = 150 mV, a practically complete Cd monolayer (Fig. 3.e) is reached, keeping the surface morphology prior to Cd UPD (Fig. 3.b). When the potential is located in the A_3 peak region, at ΔE = 100 mV, new islands nucleate onto the monolayer recently formed (see the brightest islands in Fig. 3.f), which again grow and coalesce at a constant potential. After t_p = 370 s, a second complete Cd monolayer is formed on the surface (Fig. 3.g). It is important to note that, contrary to the first Cd monolayer, the formation of the second layer changes the surface, in which some of the step edges

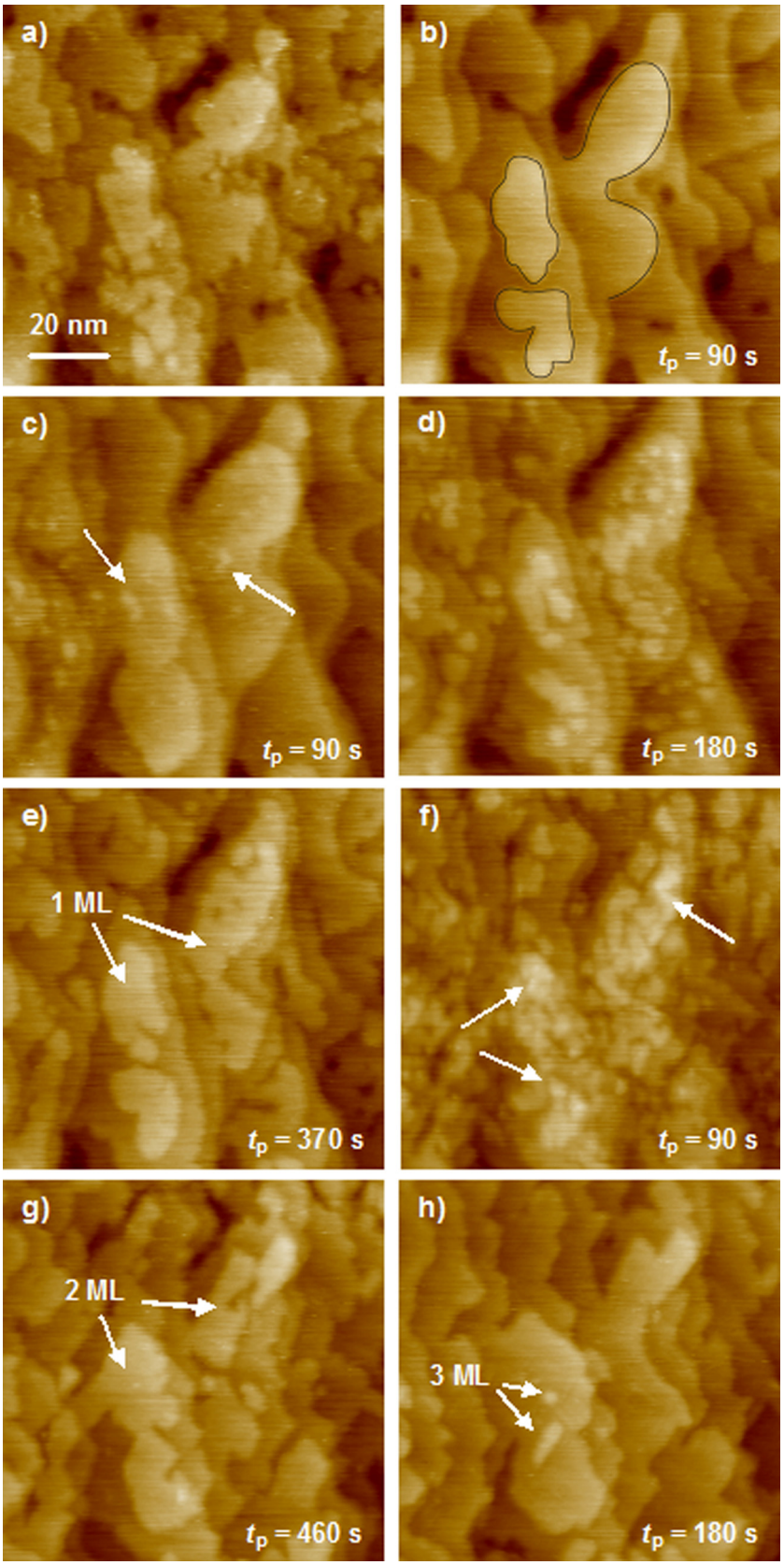

Fig. 3. In-situ STM images of the Cd underpotential deposition onto Au(100). System Au(100)/1 mM $CdSO_4$ + 5 mM H_2SO_4 + 0.1 M Na_2SO_4. a) ΔE = 1250 mV, b) ΔE = 950 mV, c-d) ΔE = 200 mV, e) ΔE = 150 mV, f-g) ΔE = 100 mV, h) ΔE = 50 mV. T = 298 K.

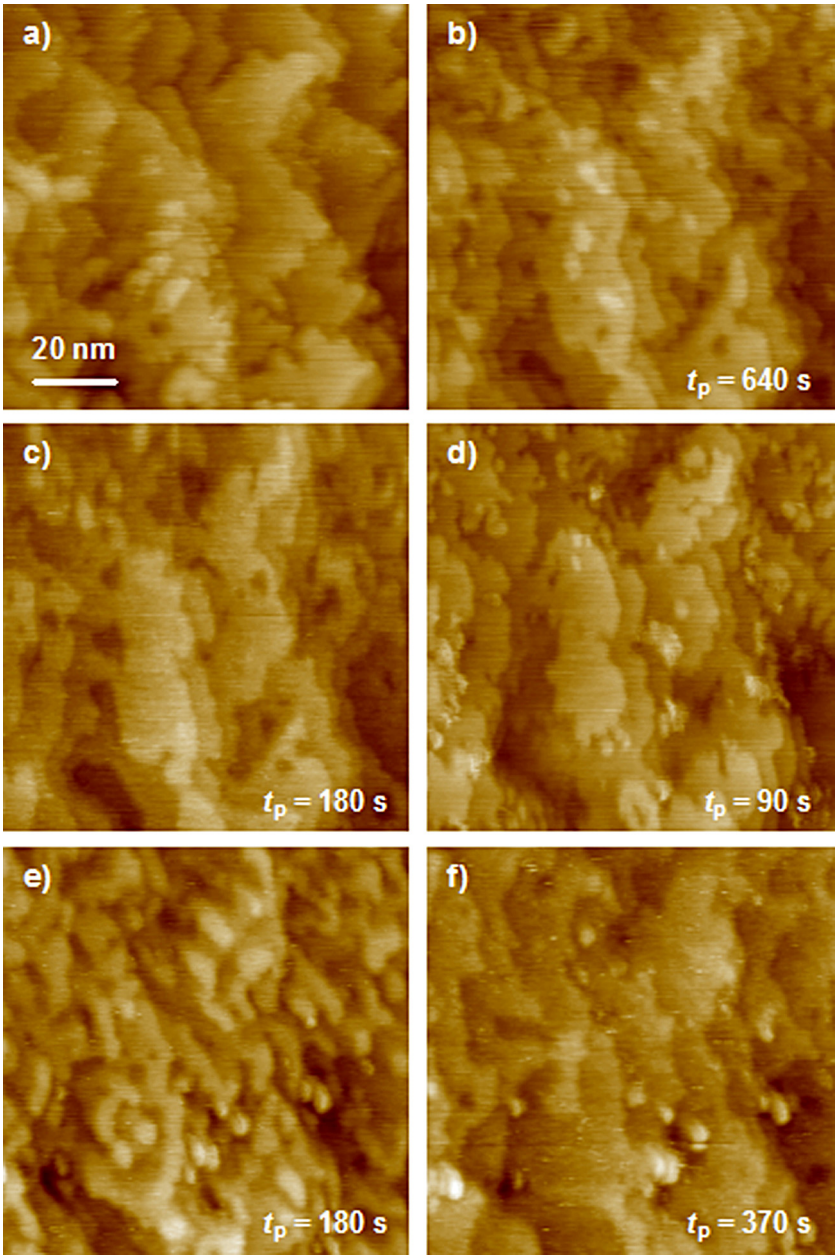

Fig. 4. In-situ STM images of the dissolution process of the Cd underpotentially deposited onto Au(100) shown in Fig. 3. System Au(100)/1 mM $CdSO_4$ + 5 mM H_2SO_4 + 0.1 M Na_2SO_4. a) ΔE = 100 mV, b) ΔE = 250 mV, c) ΔE = 350 mV, d) ΔE = 650 mV, e) ΔE = 1300 mV, f) ΔE = 1450 mV. T = 298 K.

acquire a quadratic morphology. Finally, at ΔE = 50 mV (Fig. 3.h) the beginning of a third Cd layer underpotentially deposited on Au(100) is observed. The formation of a second and third Cd monolayers at underpotentials is favoured by the fact that, probably, the underlying gold surface is being reorganized as it is covered with Cd adatoms, as was reported for the Au(111)/Cd^{2+} system [8,9,21].

The sequence of in situ STM images shown in Fig. 4 presents the changes of surface topography during the subsequent anodic stripping of the deposited Cd layers. In the underpotential range $40 < \Delta E/\text{mV} < 350$, a continuous and sequential dissolution of the third and second Cd monolayers previously deposited (peaks D_3 and D_2) takes place (Fig. 4.a-c). There are less noticeable changes in the surface morphology if the potential value exceeds that for the D_1 peak (Fig. 4.d). As seen the removal of Cd leads to an appearance of islands and pits on the terraces. This behaviour is characteristic for alloy dissolution and has been observed previously in other systems [12]. These pits disappear by changing the underpotential to more positive values suggesting a relatively high mobility of Au surface atoms. At relatively more positive potentials, ΔE = 1050 mV, a dissolution of the Cd layer is evidenced, and it is increased at even more positive potentials (ΔE = 1300 mV) (Fig. 4.e). Finally, at ΔE = 1450 mV, and for the time used in the experiment, the surface shows no appreciable changes (Fig. 4.f). The initial Au surface was not recovered and this result is an indication of a vertical atomic exchange process between the Au atoms of the substrate and Cd adatoms leading to a Au-Cd surface alloy, formed at low underpotentials (A_3 peak region). This phenomenon would allow the formation of more than one monolayer in the underpotential range. Therefore, the results obtained with in-situ STM are consistent with the desorption curves shown in Figure 2, where it was proposed the formation of a Au-Cd surface alloy and the dissolution of various Cd-Au alloy phases. In addition, the new peaks D', D" and D"' registered at very positive potential values go exactly with the observed STM images related to the last steps of the alloy dissolution, which

was formed at low underpotentials. The information provided by the integration of the circulated charge density in the long time polarization experiences, presented in the insets of Fig. 2, is also consistent with the morphology changes observed by in-situ STM.

4. Conclusions

The Cd UPD process in the system Au(100)/Cd^{2+}, SO_4^{2-} was analysed using conventional electrochemical techniques and in-situ STM analysis. Voltammetric measurements indicate that this process is characterized by three adsorption/desorption peaks pairs before the Cd bulk deposition. From long polarization time experiences, it is possible to confirm the formation of a Au-Cd surface alloy, which involves different phases, evidenced by the occurrence of additional stripping peaks. The relation between Δq and $t_p^{1/2}$ indicates a surface transformation associated with an atomic place exchange process between the Au substrate atoms and the deposited Cd atoms. For relatively long polarization times, the extent of the alloyed phase into the surface will be governed by solid state diffusion of both Cd and Au atoms through the alloy surface rich in vacancies. At lower underpotentials, Δq considerably exceeds the value of a monolayer and significantly increases with t_p, exhibiting two different behaviors with $t_p^{1/2}$, for relatively long and short polarization times. At shorter polarization times, the behavior observed is attributed to the formation of an alloy thin film by a solid state mechanism. The initial formation of this Au-Cd surface alloy is followed by a second and greater increase in the anodic charge density at higher t_p, which can be attributed to the formation of other phases of a Cd_zAu_x alloy.

STM images have shown that the Cd deposition becomes evident at low underpotentials, with the nucleation of two-dimensional islands of monatomic height, which grow and coalesce up to a complete monolayer. At lower underpotentials, the formation of a second and a third Cd monolayers was also observed in the in-situ STM images, favoured by the fact that, the underlying gold surface is being reorganized as it is covered with Cd adatoms, in agreement with kinetic results. The anodic dealloying leads to an appearance of islands and pits on the surface, which disappear at high underpotentials ($\Delta E > 1450$ mV) suggesting a relatively high mobility of surface Au atoms.

Acknowledgements

The authors wish to thank the Universidad Nacional del Sur, Argentina, for financial support of this work. M.C. del Barrio especially grateful to D.R. Salinas for his direction, support and encouragement. His memory is always present.

References

[1] J.N. Jovićević, A.R. Despić, D.M. Dražić, Studies of the deposition of cadmium on foreign substrates, Electrochim. Acta 22 (1977) 577.
[2] B.W. Gregory, D.W. Suggs, J.L. Stickney, Conditions for the Deposition of CdTe by Electrochemical Atomic Layer Epitaxy, J. Electrochem. Soc. 138 (1991) 1279.
[3] X. Xing, D.A. Scherson, C. Mak, Coverage of the Cd Underpotential Deposited Layer Formed on an Au(111) Substrate, J. Electrochem. Soc. 149 (2002) C586.
[4] S. Hsieh, A.A. Gewirth, Nitrate Reduction Catalyzed by Underpotentially Deposited Cd on Au(111), Langmuir 16 (2000) 9501.
[5] J.W. Schultze, F.D. Koppitz, M.M. Lohrengel, Elektrochemische Untersuchungen zur Festkörperdiffusion: Adsorption und Legierungsbildung im System Gold/Cadmium, Ber. Bunsenges. Phys. Chem. 78 (1974) 693.
[6] J.C. Bondos, A.A. Gewirth, R.G. Nuzzo, Observation of Uniaxial Structures of Underpotentially Deposited Cadmium on Au(111) with in Situ Scanning Tunneling Microscopy, J. Phys. Chem. 100 (1996) 8617.
[7] B.K. Niece, A.A. Gewirth, Potential-Step Chronocoulometric and Quartz Crystal Microbalance Investigation of Coadsorbed Cadmium and Sulfate on Au(111) Electrodes, Langmuir 13 (1997) 6302.
[8] G. Inzelt, G. Horányi, On the alloy formation in the course of upd of Cd on gold, J. Electroanal. Chem. 491 (2000) 111.
[9] M.C. del Barrio, S.G. García, C.E. Mayer, D.R. Salinas, New insights on the Cd UPD on Au(111), Surf. and Interface Anal. 40 (2008) 22.
[10] R. Vidu, S. Hara, In situ EC-AFM observation of Cd electrodeposition on Au(100), Scr. Mater. 41 (1999) 617.
[11] R. Vidu, S. Hara, Surface alloying at the Cd/Au(100) interface in the upd region. Electrochemical studies and in situ EC-AFM observation, J. Electroanal. Chem. 475 (1999) 171.
[12] R. Vidu, S. Hara, Diffusion at Au(100)/Cd^{2+} interface during electrodeposition, Surf. Sci. 452 (2000) 229.
[13] R. Vidu, S. Hara, Comparative kinetic study of Cd diffusion into Au(100) and Ag(100) during electrodeposition, Phys. Chem. Chem. Phys. 3 (2001) 3320.
[14] R. Vidu, S. Hara, In situ electrochemical atomic force microscopy study on Au(100)/Cd interface in sulfuric acid solution, J. Vac. Sci. Technol. B 17 (1999) 2423.
[15] K. Engelsmann, W.J. Lorenz, E. Schmidt, Underpotential deposition of lead on polycrystalline and single-crystal gold surfaces: Part I. Thermodynamics, J. Electroanal. Chem. 114 (1980) 1.
[16] S.G. García, D.R. Salinas, C.E. Mayer, J.R. Vilche, H.-J. Pauling, S. Vinzelberg, G. Staikov, W.J. Lorenz, Silver electrodeposition on Au(100): structural aspects and mechanism, Surf. Sci. 316 (1994) 143.
[17] E. Budevski, G. Staikov, W.J. Lorenz, Electrocrystallization Nucleation and growth phenomena, Electrochim. Acta 45 (2000) 2559.
[18] S.G. García, D.R. Salinas, G. Staikov, Underpotential deposition of Cd on Ag(111): an in situ STM study, Surf. Sci. 576 (2005) 9.
[19] M.C. del Barrio, S.G. García, D.R. Salinas, Alloy formation in the system Au(111)/Cd during the UPD process, Electrochem. Commun. 6 (2004) 762.
[20] N. Ikemiya, M. Nishide, S. Hara, Potential dependence of the surface self-diffusion coefficient on Au(100) in sulfuric acid solution measured by atomic force microscope, Surf. Sci. 340 (1995) L965.
[21] S. Maupai, Y. Zhang, P. Schmuki, Nanoscale observation of initial stages of Cd-electrodeposition on Au(111), Surf. Sci. 527 (2003) L165.